Journal of
Ceramic Science
and Technology

J. Ceram. Sci. Tech., 07 [04] 469-476 (2016)
DOI: 10.4416/JCST2016-00063
available online at: http://www.ceramic-science.com

Short Communication

Crystallization Behavior, Microstructure and Magnetic Properties of B_2O_3-SiO_2-Fe_2O_3-BaO-SrO Glass-Ceramics

M. Tavoosi*, A. Ghasemi, D. Yousefi

Department of Materials Engineering, Malek-Ashtar University
of Technology (MUT), Shahin-Shahr, Isfahan, Iran.

received August 30, 2016; received in revised form November 12, 2016; accepted November 22, 2016

Abstract

The preparation and magnetic characterization of B_2O_3-SiO_2-Fe_2O_3-BaO-SrO glass-ceramics were the goal of this study. In this regard, different mixtures of B_2O_3, SiO_2, Fe_2O_3, BaO and SrO were melted in the temperature range 1200 – 1350 °C and were quenched between two sheets of cold steel. The as-quenched samples were annealed at 660 and 700 °C for 2 h. The prepared samples were then characterized using X-ray diffraction (XRD), field emission scanning electron microscopy (FESEM), differential scanning calorimetry (DSC) and a vibrating scanning magnetometer (VSM). According to the results obtained, fully amorphous phase can be formed in the $20B_2O_3$-$10SiO_2$-$25Fe_2O_3$-45BaO, $20B_2O_3$-$10SiO_2$-$25Fe_2O_3$-45SrO and $20B_2O_3$-$10SiO_2$-$25Fe_2O_3$-22.5BaO-22.5SrO systems. The coercivity and saturation of magnetizationof the as-quenched amorphous samples were estimated at about 120 – 380 Oe and 9 – 12 emu/g, respectively. The coercivity value increased during the annealing process as a result of precipitation of hard magnetic $MFe_{12}O_{19}$ phase from the amorphous matrix. Although, all of samples showed almost the same saturation of magnetization, the highest value of coercivity (4620 Oe) was achieved in $20B_2O_3$-$10SiO_2$-$25Fe_2O_3$-22.5SrO-22.5BaO sample with simultaneous presents of Sr and Ba.

Keywords: Glass-ceramics, crystallization, magnetic materials, hexaferrite.

I. Introduction

The magnetic properties of amorphous materials containing transition metal ions have been studied extensively in the past for both practical and fundamental reasons [1–5]. Considerable interest has been shown in iron-bearing oxide glasses because of their interesting magnetic, structural and optical properties [5–9]. The glass crystallization of iron-bearing oxide glasses is commonly employed to produce various magnetic materials such as $SrFe_{12}O_{19}$ and $BaFe_{12}O_{19}$ with optimum magnetic properties [10,11]. The interest in magnetic glass-ceramics arises from the great potential for application, which includes magnetic storage devices, Magnetic Resonance Imaging (MRI) contrasting agents, magnetic hyperthermia, bio-detection, microwave devices and waste sorbent [1].

Owing to their superior properties, barium and strontium hexaferrites have been utilized in various applications as permanent magnets and particulate media for recording high-density information [12–17]. Most investigators have chosen B_2O_3 and SiO_2 as glass formers and Fe_2O_3, BaO and SrO as magnetic phase formers for their base glass composition. The effects of compositions, nucleating agents and annealing treatment on the magnetic properties of prepared glass-ceramics have been reported by these researchers. For instance, Mirkazemi *et al.* [13] prepared a $BaFe_{12}O_{19}/BaB_2O_4$ composite microstructure with optimum magnetic properties in the BaO-Fe_2O_3-B_2O_3-SiO_2 system (H_c = 2800 Oe and M_s = 26 emu/g). The optimum annealing temperature and time in this study was 720 °C and 1 h, respectively. The effect of SiO_2 and Cr_2O_3 additions on the crystallization behavior and magnetic properties of a B_2O_3-BaO-Fe_2O_3 glass system has also been investigated by Marghussian *et al.* [17]. This study showed that with modification of initial composition, the coercivity value can increase to above 4000 Oe. The annealing conditions in this study were T = 723 °C and t = 1 h. Preparation of multiferroic BaO-Y_2O_3-Fe_2O_3-Nb_2O_5 glass-ceramic has also been investigated by Wu *et al.* [18]. The maximum coercivity and saturation of magnetizationin this study were about 2100 Oe and 1.6 emu/g, respectively.

As maintained above, a lot of investigations have been undertaken into the formation and magnetic characterization of different magnetic glass-ceramics [10–16]. However, the exact effects of BaO and SrO on the structural and magnetic properties of the B_2O_3-SiO_2-Fe_2O_3 system have not been properly investigated. Therefore, the preparation and magnetic characterization of B_2O_3-SiO_2-Fe_2O_3-BaO-SrO glass-ceramics were the goal of this study. In fact, the formation of B_2O_3-SiO_2-Fe_2O_3-BaO-SrO glass-ceramics with the highest value of coercivity, during crystallization process, is the major novelty of this work.

* Corresponding author: ma.tavoosi@gmail.com

II. Materials and Methods

H_3BO_3 (Merck, 99.8 % purity, 1 mm), SiO_2 (Merck, 99.8 % purity, 250 μm), $BaCO_3$ (Merck, 99.8 % purity, 2 mm), $SrCO_3$ (Merck, 99.8 % purity, 350 μm) and Fe_2O_3 (Merck, 99.8 % purity, 100 μm) were used as raw materials. Different compositions of B_2O_3-SiO_2-Fe_2O_3-BaO-SrO, based on Table 1 (with total weight of 30 g), were melted in a temperature range of 1200 – 1350 °C for 1 h and then quenched between two cold steel sheets (with a high cooling rate). It is important to note that the total percentage of glass formers (B_2O_3+SiO_2) and MO/Fe_2O_3 (M=Ba, Sr, Ba+Sr) ratio in this composition were chosen at 30 mol% and 25/45, respectively. This selection was made based on Marghussian *et al.* [17] and our previous study [5]. As-quenched samples were stress-relieved at about 30 °C below the glass transition temperature for 2 h and slowly cooled down to room temperature. The annealing procedure was performed at 660 and 700 °C for 2 h in ambient atmosphere. These annealing conditions were chosen based on DSC results (according to the crystallization temperature of prepared glasses).

Table. 1: The chemical composition of B_2O_3-SiO_2-Fe_2O_3-BaO-SrO glass-ceramics.

Sample Number S.N.	Chemical Composition (mol%)				
	B_2O_3	SiO_2	Fe_2O_3	BaO	SrO
1	20	10	25	45	-
2	20	10	25	-	45
3	20	10	25	22.5	22.5

The XRD technique using a diffractometer with Cu Kα radiation (λ = 0.15406 nm; 40 kV; Philips PW3710) was used to follow the structural variation of the specimens (2θ range: 10 – 80°, step size: 0.05°; time per step: 1 s). The mean crystal sizes were estimated from broadening of X-ray peaks according to Scherrer's equation [18]:

$$D = K\,\lambda/\Delta(2\theta)\cos\theta \qquad (1)$$

where λ is the wavelength of X-ray radiation, θ is the diffraction angle, Δ(2θ) is the width of the peak at half of its maximum, and K is a dimensionless number known as the Scherrer constant. K generally depends both on the shape of the crystal particles and on the order of XRD spectrum (in the case of spherical particles, K is equal to 1.0747).

Structural and morphological characterizations of samples were conducted by means of field emission scanning electron microscopy (VEGA-TESCAN-XMU) at an accelerating voltage of 15 kV. This microscope was equipped with a detector for energy-dispersive X-ray (EDS) analyses. Before the SEM investigation, the specimens were polished and etched in 0.5 % HF for 75 s and then were coated with Au. Differential scanning calorimetry was also conducted to study the thermal stability of the prepared samples using the Linseis Thermal Balance L81/1750 DTA differential thermal analyzer. The samples were placed in Al_2O_3 pans and heated in a dynamic argon atmosphere up to 900 °C at a heating rate of 20 °C/min. The magnetic properties of the prepared samples were measured using a vibrating scanning magnetometer (VSM) under an applied field up to 15 kOe.

III. Results and Discussion

The XRD patterns of B_2O_3-SiO_2-Fe_2O_3-BaO-SrO as-quenched samples are presented in Fig. 1. On the basis of these XRD patterns, the microstructures of different specimens are completely amorphous.

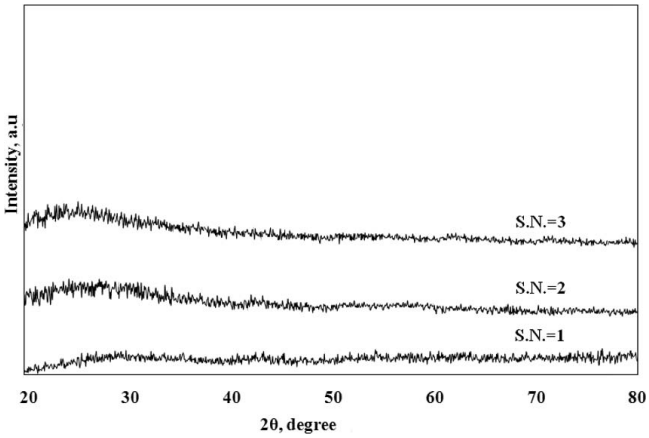

Fig. 1: XRD patterns of B_2O_3-SiO_2-Fe_2O_3-BaO-SrO as-quenched samples.

The hysteresis loops and magnetic properties of as-quenched samples are presented in Table 2. Unexpectedly, the fully glassy samples exhibit ferromagnetic behavior. However, when the glass does not contain crystalline Fe-rich precipitates, it exhibits paramagnetic properties. This indicates that the microstructure of the as-quenched samples is not fully amorphous and consists of magnetic crystalline phases that are not detectable by means of XRD analysis. The coercivity (H_c) and saturation of magnetization (M_s) of the as-quenched samples are in the range of about 120 – 380 Oe and 9 – 12 emu/g, respectively. In fact, amorphous materials have no grains and grain boundaries; and during solidification processes most impurities tend to remain in solution rather than precipitating out. In these materials, the defects (grain boundaries, interphase boundaries and second-phase precipitates) have low pinning effects on the movement of the domain walls [19, 20] and they have low coercivity.

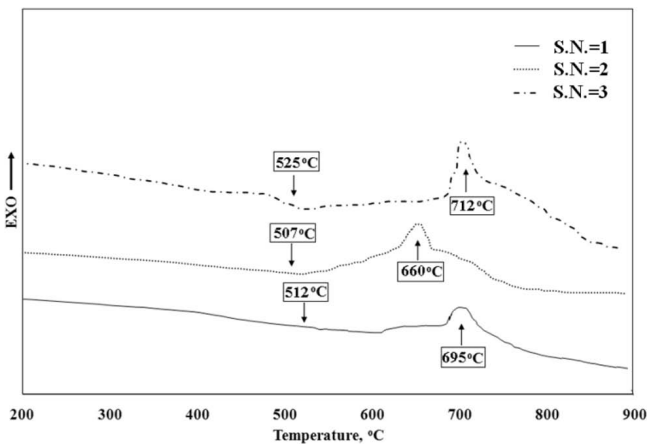

Fig. 2: DSC heating traces of B_2O_3-SiO_2-Fe_2O_3-BaO-SrO as-quenched samples.

Table. 2: The DSC results and the crystallization products in as-quenched samples after annealing at 700 °C for 2 h.

S.N.	Hysteresis Loops	Magnetic properties	
		M_s (emu/g)	H_c (Oe)
1	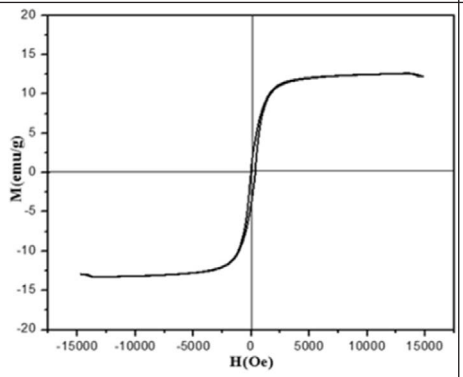	12	120
2	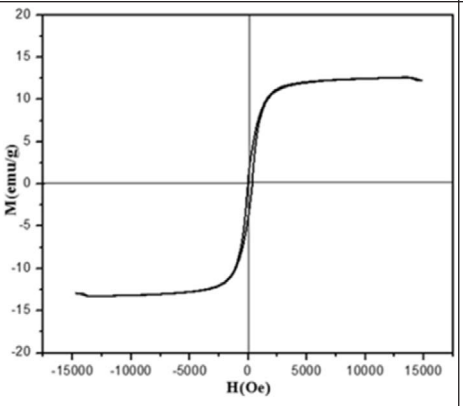	12	95
3	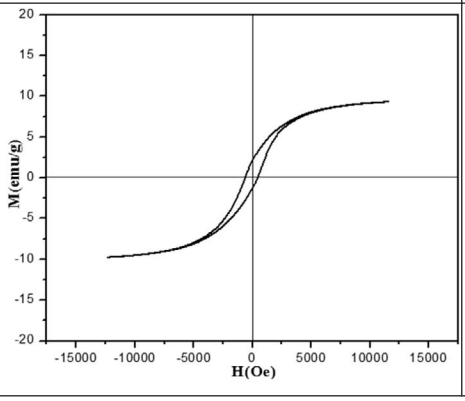	9	380

The DSC heating traces of different prepared samples are presented in Fig. 2. It can be seen that general characterizations of these DSC curves are the same and only one change in the slope of the base line and one exothermic peak appear in these curves. In fact, the change in the slope of the base line in these curves is related to the glass transition temperature (T_g). To analyze the crystallization process responsible for the exothermic peak (crystallization temperature, T_c), the samples were annealed at 700 °C for 2 h. Although, the crystallization temperature of S.N.=2 is lower (about 660 °C) than that of the other specimens, for better comparison, the annealing process for different samples was performed with the same conditions.

The XRD patterns of annealed samples are presented in Fig. 3. Moreover, the SEM micrographs and EDS results of precipitated compounds in different samples are also shown in Figs. 4 and 5, respectively. It can be seen that the microstructure of as-quenched samples in different systems is the same and consists of $MFe_{12}O_{19}$ and $M_2FeSi_2O_7$ (M = Ba, Sr) phases (Table 3). So, the exothermic peaks in DSC curves can be attributed to precipitation of these phases from the amorphous matrix. According to Fig. 4 (a), the microstructure of the S.N.=1 consists of needle-shaped $BaFe_{12}O_{19}$ precipitates (measuring 100 nm in diameter and 500 nm in length) which were dispersed in the $Ba_2FeSi_2O_7$ matrix. When barium is replaced with strontium (S.N.=2 and S.N.=3), the morphology of $MFe_{12}O_{19}$ phase changes to a spherical shape (with average particle size of about 100 nm (Fig. 4 (b) and (c)).

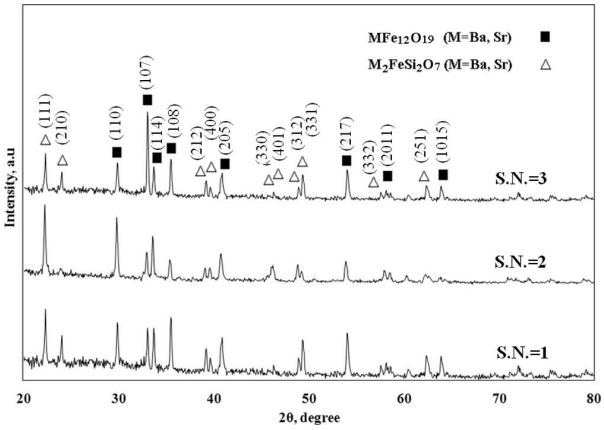

Fig. 3: XRD patterns of B_2O_3-SiO_2-Fe_2O_3-BaO-SrO as-quenched samples after annealing at 700 °C for 2 h.

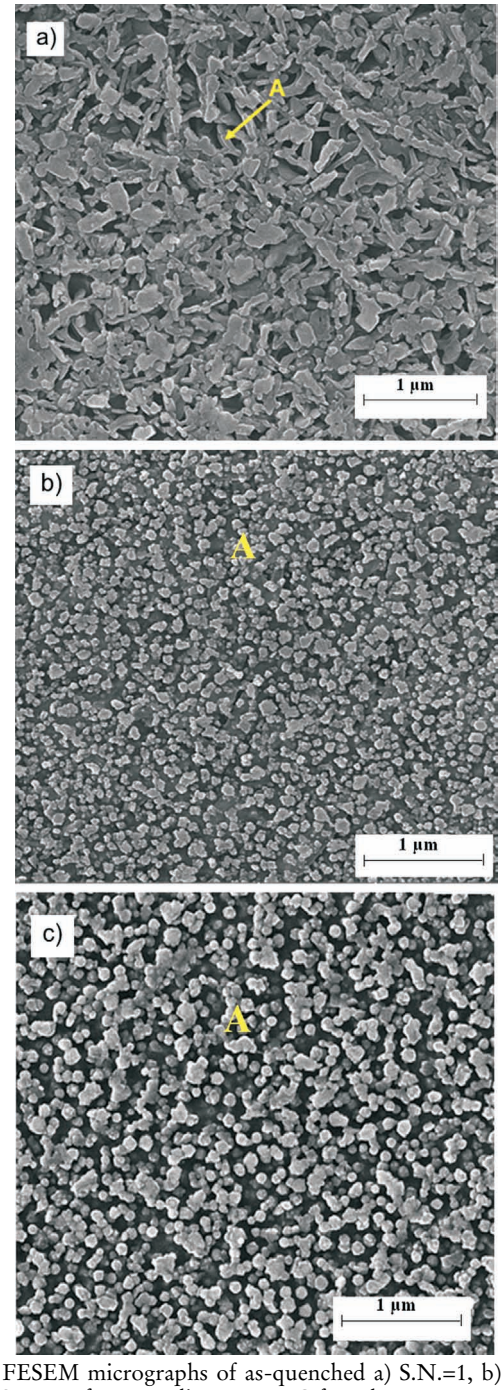

Fig. 4: FESEM micrographs of as-quenched a) S.N.=1, b) S.N.=2 and c) S.N.=3 after annealing at 700 °C for 2 h.

Although the total crystallization sequences of different specimens are similar, T_g, T_c and ΔT ($\Delta T = T_c - T_g$) in these three systems differ from each other (Table 3). These results demonstrate that the crystallization temperature of produced amorphous phases is in the range of 660 to 700 °C and decreases in the order of S.N=3 > S.N= 1 > S.N=2.

Table 3: The hysteresis loops and magnetic properties of as-quenched samples.

S.N.	Crystallization products	T_g (°C)	T_c (°C)	ΔT (T_c-T_g)
1	$BaFe_{12}O_{19}$, $Ba_2FeSi_2O_7$	512	695	183
2	$SrFe_{12}O_{19}$, $Sr_2FeSi_2O_7$	507	660	153
3	$MFe_{12}O_{19}$ (M=Ba,Sr), $M_2FeSi_2O_7$ (M=Ba,Sr)	525	712	187

Table 4 summarizes the hysteresis loops and magnetic properties of the final samples, which have been investigated according to DSC results. Based on these results, several points can be concluded:

- Regardless of the chemical composition and annealing temperature, there is no significant differences between the magnetic properties of all the final samples.
- The hysteresis loops of the samples after the annealing process exhibit an almost suitable squareness ratio. In fact, high magneto-crystalline anisotropy of $MFe_{12}O_{19}$ has an impact on the magnetization reversal mechanism named by Stoner-Wohlfarth or domain wall movement and high square ratio in hysteresis loops [19]. However, the kink in the hysteresis loops can be related to the formation of soft magnetic Fe-oxides phases in annealed samples (which is not detectable with the XRD technique).
- With annealing of the produced samples, the saturation of the magnetization value increases and reaches about 22 – 25 emu/g. In fact, the theoretical value of M_s for barium and strontium hexaferrite single crystals is about 72 emu/g [16]. It can be concluded that the measured M_s in this work is about 30 % of the theoretical value. In fact, these differences can be related to the formation of non-magnetic $M_2FeSi_2O_7$ phase during the annealing process. The saturation of magnetization depends on the number of aligned spins per unit value. Precipitation of $M_2FeSi_2O_7$ phase during annealing reduces the volume percentage of barium and strontium hexaferrite. In consideration of this point, it is clear that the saturation of magnetization value of glass-ceramics be lower than that of pure M-type hexaferrites.
- Like the saturation of magnetization, the coercivity value of the produced samples increases during annealing. In fact, this phenomenon stems from an increase in the percentage of hard magnetic phases and pinning of the magnetic domain walls. According to the above, annealing the as-quenched samples leads to the precipitation of $MFe_{12}O_{19}$ phase from the amorphous matrix. Developing the $MFe_{12}O_{19}$ hard magnetic phase with high magneto-crystalline anisotropy and large

anisotropy constant is the main reason for the increase in the coercivity value in the annealed samples [20].

– In contrast to the saturation of magnetization, the coercivity values of glass-ceramics decreases in the order of S.N.=3>S.N.=1>S.N.=2. On the other hand, the $20B_2O_3$-$10SiO_2$-$25Fe_2O_3$-22.5BaO-22.5SrO sample, with simultaneous presence of Sr and Ba, shows a higher coercivity value than other systems studied in this work and the values reported by Shirk [12], Zaitsev [13], Mekki [14], Yousefi [5] and Mirkazemi [15] (lower than 3500 Oe). In fact, the coercivity is linearly related to the reciprocal of crystallite size and also is dependent on magnetocrystalline anisotropy as shown by the following equation[20]:

$$H_c = 2K_1/M_s \quad (2)$$

where K_1 is the magnetic anisotropy constant and M_s is the saturation of magnetization. Consequently, it is concluded that with decreasing crystallite size, the coercivity is increased. Based on XRD measurements (Table 5) and VSM results (Table 4), the crystallite sizes and M_s values of different samples in this study are the same. So, based on Eq. (2), the higher coercivity value of $20B_2O_3$-$10SiO_2$-$25Fe_2O_3$-22.5BaO-22.5SrO glass-ceramic can be related to the anisotropy constant. However, further studies are needed to confirm this.

Table 4: The hysteresis loops and magnetic properties after the annealing treatment.

S.N.	660 °C			700 °C		
	Hysteresis Loops	M_s (emu/g)	H_c (Oe)	Hysteresis Loops	M_s (emu/g)	H_c (Oe)
1	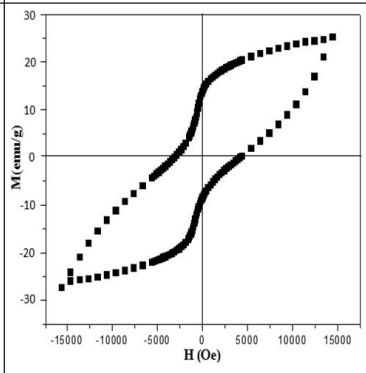	23	2950	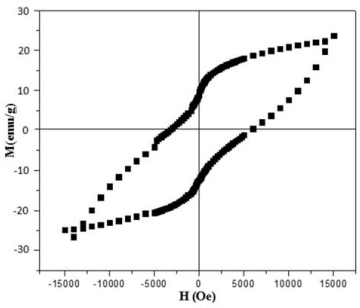	22	3100
2	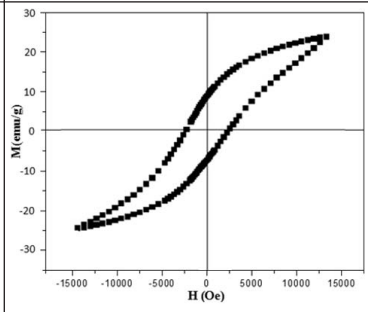	22.5	2570	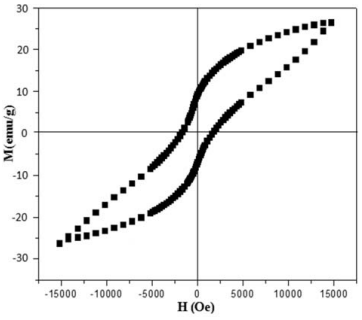	23.58	2600
3	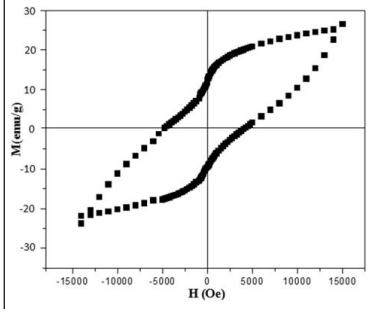	25.7	4180	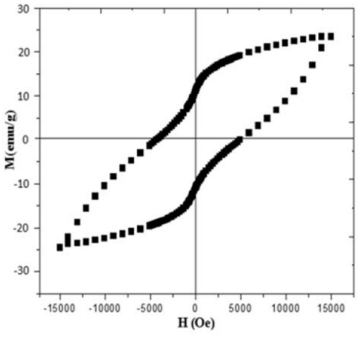	24.65	4620

Table 5: The crystallite size of the new phases in the annealed samples.

S.N	Phase	Crystallite size, (nm)	
		660 °C	700 °C
1	$BaFe_{12}O_{19}$	80	88
	$Ba_2FeSi_2O_7$	18	25
2	$SrFe_{12}O_{19}$	73	76
	$Sr_2FeSi_2O_7$	22	28
3	$MFe_{12}O_{19}$ (M=Ba,Sr)	89	85
	$M_2FeSi_2O_7$ (M=Ba,Sr)	29	30

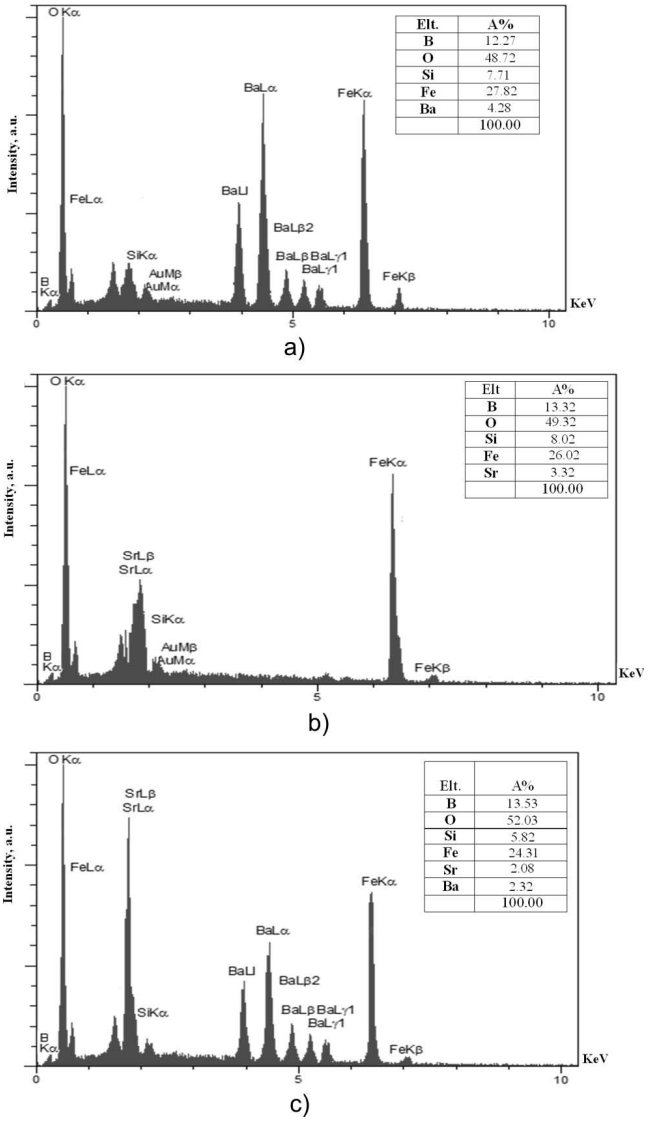

Fig. 5: EDS analysis of precipitate compounds in as-quenched a) S.N.=1, b) S.N.=2 and c) S.N.=3 after annealing at 700 °C for 2 h.

IV. Conclusion

The preparation and magnetic characterization of B_2O_3-SiO_2-Fe_2O_3-BaO-SrO glass-ceramics were the goal of this study. The results obtained showed that fully amorphous phase can be formed in $20B_2O_3$-$10SiO_2$-$25Fe_2O_3$-45MO(M=Ba, Sr) systems. The coercivity and saturation of magnetizationof as-quenched samples were estimated at about 120 – 380 Oe and 9 – 12 emu/g, respectively. With annealing of the produced specimens, the coercivity value increased as a result of precipitation of hard magnetic $MFe_{12}O_{19}$ phase in the nonmagnetic $M_2FeSi_2O_7$ matrix. Although all the annealed samples showed almost the same saturation of magnetization, the highest value of coercivity (4620 Oe) was achieved in the $20B_2O_3$-$10SiO_2$-$25Fe_2O_3$-22.5SrO-22.5BaO system with simultaneous presence of Sr and Ba.

References

1 Sandu, V., Nicolescu, M.S., Kuncser, V., Damian, R., Sandu, E.: Magnetic glass-ceramics, *J. Adv. Ceram.*, **1**, 138 – 143, (2012).

2 Perry, C.H., Kinser, D.L., Wilson, L.K., Vaughn, J.G.: Magnetic exchange between Ti^{3+} ions in titanium phosphate glass, *J. Appl. Phys.*, **50**, 1601 – 1603, (1979).

3 Hu, F., Wei, X., Qin, Y., Jiang, S., Li, X., Zhou, S., Chen, Y., Duan, C.K., Yin, M.: Yb^{3+}/Tb^{3+} co-doped $GdPO_4$ transparent magnetic glass-ceramics for spectral conversion, *J. Alloy. Compd.,* **674**, 162 – 167, (2016).

4 Freibele, E.J., Koon, N.C.: Magnetization studies of amorphous antiferromagnetism in manganese phosphate glass, *Solid State Commun.*, **14**, 1247 – 1250, (1974).

5 Yousefi, D., Tavoosi, M., Ghasemi, A.: Magnetic properties of B_2O_3-SiO_2-BaO-Fe_2O_3 glass-ceramics, *J. Non-Cryst. Solids,* **443**, 1 – 7, (2016).

6 Ardelean, I., Ilonca, Gh., Peteanu, M., Pop, D.: Magnetic properties of $x \cdot MnO \cdot (1\text{-}x)\,[19TeO_2 \cdot PbO]$ glasses, *Solid State Commun.*, **3**, 635 – 655, (1980).

7 Tanaka, K., Nakahara, Y., Hirao, K., Soga, N.: Preparation and magnetic properties of glass-ceramics containing magnetite microcrystals in calcium iron aluminoborate system, *J. Magn. Magn. Mater.,* **168**, 203 – 212, (1997).

8 Woltz, S., Hiergeist, R., Görnert, P., Rüssela, C.: Magnetite nanoparticles prepared by the glass crystallization method and their physical properties, *J. Magn. Magn. Mater.,* **298**, 7 – 13, (2006).

9 Abdel-Hameed, S.A.M., Hessien, M.M., Azooz, M.A.: Preparation and characterization of some ferromagnetic glass-ceramics contains high quantity of magnetite, *Ceram. Int.*, **35**, 1539 – 1544, (2009).

10 Sohn, S.B., Choi, S.Y., Shim, I.B.: Preparation of Ba-ferrite containing glass-ceramics in BaO-Fe_2O_3-SiO_2, *J. Magn. Magn. Mater.,* **239**, 533 – 536, (2002).

11 Müller, R., Ulbrich, C., Schüppel, W., Steinmetz, H.: Preparation and properties of barium-ferrite-containing glass-ceramics, *J. Eur. Ceram. Soc.,* **19**, 1547 – 1550, (1999).

12 Shirk, B.T., Buessem, W.R.: Temperature dependence of ms and K_1 of $BaFe_{12}O_{19}$ and $SrFe_{12}O_{19}$ single crystals, *Jpn. J. Appl. Phys.*, **40**, 1294 – 1296, (1969).

13 Zaitsev, D.D., Kazin, P.E., Garshev, A.V., Tretyakov, Y.D., Jansen, M.: Synthesis and magnetic properties of SrO-Fe_2O_3-B_2O_3 glass-ceramics, *Inorg. Mater.*, **40**, 881 – 885, (2004).

14 Mekki, A.: Magnetic properties of Fe ions in a silicate glass and ceramic, *physica status solidi,* **184**, 327 – 333, (2001).

15 Mirkazemi, M., Marghussian, V.K., Beitollahi, A.: Crystallization behaviour, microstructure and magnetic properties of BaO-Fe_2O_3-B_2O_3-SiO_2 glass-ceramics, *Ceram. Int.*, **32**, 43 – 51, (2006).

16 Rathenau, G.W.: Saturation and magnetization of hexagonal iron oxide compound, *Rev. Mod. Phys,* **25**, 297 – 302, (1953).

[17] Marghussian, V.K., Beitollahi, A., Haghi, M.: The effect of SiO_2 and Cr_2O_3 additions on the crystallization behavior and magnetic properties of a B_2O_3-BaO-Fe_2O_3 glass, *Ceram. Int.*, **29**, 455 – 462, (2003).

[18] Cullity, B.D.: Elements of X-ray diffraction, 2nd edition, Addison Wesley, 1978.

[19] Shirk, B.T., Buessem, W.R.: Magnetic properties of barium ferrite formed by crystallization of glass, *J. Am. Ceram. Soc.*, **53**, 192 – 196, (1970).

[20] Cullity, B.D., Graham, C.D.: Introduction to magnetic materials, 2nd edition, JohnWilley & Sons, Inc., Hoboken, New Jersey, 2009.